Transition-metal acceptor complexes in zinc oxide

M. A. Gluba and N. H. Nickel

Helmholtz-Zentrum Berlin für Materialien und Energie, Institut für Silizium-Photovoltaik, Kekuléstrasse 5, D-12489 Berlin, Germany

(Received 23 February 2012; published 15 February 2013)

The incorporation of hydrogen shallow donors gives rise to Mn^{2+} fine and hyperfine lines in the electron paramagnetic resonance of ZnO. This cannot be explained by recharging of isolated Mn atoms. First-principles density functional calculations reveal that transition metals readily form complexes with acceptors by a charge-transfer process or by bond formation. This mechanism has implications on both complex partners. Acceptors are neutralized and uncommon charge states of the transition metals are stabilized. Implications for dilute magnetic ZnO are discussed.

DOI: 10.1103/PhysRevB.87.085204 PACS number(s): 75.50.Pp, 71.20.−b, 76.30.−v

I. INTRODUCTION

Diluted magnetic semiconductors (DMS) enable us to use the electron spin as a novel information carrier for spintronic devices. Applications range from data storage and manipulation via spin switching to light emission with controlled polarization.[1] These outstanding functionalities are enabled by the long-range ferromagnetic interaction between foreign spins mediated by free charge carriers in a nonmagnetic matrix. Triggered by mean-field calculations, a great deal of experimental and theoretical effort was focused on transition-metal doped ZnO anticipating Curie temperatures (T_C) well above 300 K.[2]

Despite the ability of electrons *and* holes to mediate the ferromagnetic order, current high-T_C ZnO is mostly based on *n*-type material.[3–6] One of the possible routes to room-temperature ferromagnetism was proposed by Pemmaraju *et al.*,[7] who suggest complex formation of Co with intrinsic donor-type defects such as V_O and Zn_i. In addition, post-treatment in an electron and hole donating environment has proven to establish and degrade ferromagnetic interaction, respectively. Obstacles for achieving hole-mediated ferromagnetic ZnO are twofold. In contrast to *n*-type ZnO, acceptor doping suffers from an exceedingly low doping efficiency.[8] Although transition metals can be easily incorporated into ZnO, achieving the necessary hole concentration turns out to be difficult. On the other hand, if transition metals and acceptors are both present in ZnO, they tend to form complexes.

We demonstrate that transition metals (TM) and acceptors strongly interact in ZnO. The formation of a TM acceptor complex is accompanied by a charge transfer from the TM 3*d* into the acceptor valence states. This mechanism of acceptor compensation contradicts the concept of hole-mediated ferromagnetism in ZnO counteracting a high Curie temperature in this type of material. This hitherto unexpected behavior was investigated by electron paramagnetic resonance (EPR) measurements on Mn-doped ZnO. We show that additional electrons introduced into ZnO by hydrogenation change the charge state from Mn^{3+} to Mn^{2+}, which gives rise to a characteristic EPR signal. However, the Mn^{3+} charge state should never be stable since the Mn 3*d* orbitals reside close to the valence band. Hence, isolated Mn cannot explain the hydrogen-induced resonance. Calculations show that complex formation of the TM with acceptors stabilizes the Mn^{3+} charge state.

II. HYDROGEN-INDUCED EPR

X-band continuous-wave EPR measurements were performed on commercially available pressurized-melt grown ZnO single crystals with *c*-axis orientation. Spectra were obtained from samples in the as-grown state and after an additional hydrogen treatment at a temperature of 5 K. The incorporation of hydrogen or deuterium was achieved by sealing the samples in quartz ampoules with 800 mbar of hydrogen or deuterium gas. Then the ampoules were annealed at a temperature of 830 °C for 2.5 h, allowing hydrogen (deuterium) to diffuse throughout the sample. Subsequently, they were quenched to room temperature freezing a hydrogen (deuterium) concentration of about 10^{18} cm^{-3} in the crystal.

In Fig. 1, EPR spectra of as-grown, hydrogenated, and deuterated ZnO are shown. The spectra exhibit a pronounced resonance at $g = 1.956$, which is intensified by the hydrogen (deuterium) treatment. This resonance is due to shallow O-H donors.[9] In addition, the introduction of hydrogen and deuterium results in the observation of a variety of new lines over a large magnetic field scale [Figs. 1(b) and 1(c)]. Analyzing the structure of the spectrum, the new lines can be combined into five fine-split groups around $g = 2.001$, each consisting of six hyperfine lines. This implicates a center with an electron spin of $S = \frac{5}{2}$ and a nuclear spin of $I = \frac{5}{2}$. Previously, this center was identified as Mn^{2+}.[10,11]

To verify the assignment, the rotation pattern of the EPR signal was recorded. A comparison of the measured line positions with the characteristic transitions of an $S = I = \frac{5}{2}$ center is shown in Fig. 2. The resonance positions were simulated with EASYSPIN by Stoll *et al.*[12] according to the model Hamiltonian

$$H = \mu_B B_0 \mathbf{g} S + S\mathbf{A}I + S\mathbf{D}S, \tag{1}$$

where μ_B denotes the Bohr magneton, B_0 is the external magnetic field, and $\mathbf{g}$, $\mathbf{A}$, and $\mathbf{D}$ are the tensors of Zeeman, hyperfine, and zero-field interaction, respectively.

Fitting the transitions of the model Hamiltonian to the measured resonance positions reveals a center with axial symmetry whose tensors are characterized by $g_\parallel = 2.001$, $g_\perp = 2.002$, $D = 243$ G, $A_\parallel = 80.3$ G, and $A_\perp = 79.9$ G. These values are in agreement with earlier studies on Mn in ZnO.[13] Spin counting yielded a Mn concentration of 6×10^{13} cm^{-3}.

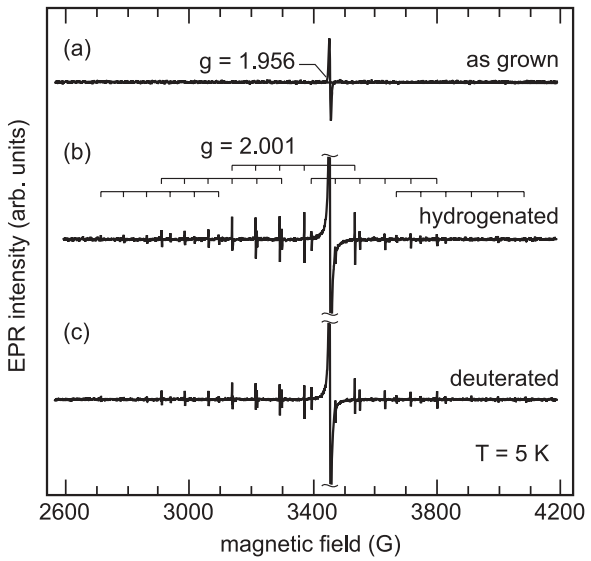

FIG. 1. EPR spectra of untreated (a), hydrogenated (b), and deuterated (c) single-crystal ZnO recorded with the crystal c axis perpendicular to the magnetic field. The untreated sample shows the H-related signal at $g = 1.956$. In addition, a fine and hyperfine split Mn^{2+} resonance is observed after hydrogenation (deuteration) (b, c).

The Mn^{2+} resonance is observed only after hydrogenation, suggesting that the formation of an Mn-H complex gives rise to the appearance of the EPR lines. When hydrogen is replaced with deuterium, the hyperfine interaction should result in a different spectrum since the nuclear spin of deuterium is $I = 1$. However, deuteration of ZnO results in exactly the same EPR spectrum as hydrogenation, clearly indicating that the formation of an Mn-H complex can be ruled out.

It is important to note that the spectra measured after hydrogenation (deuteration) are not stable. The intensity of the EPR lines decreases with time at temperatures as low as 300 K.[11] In ZnO hydrogen acts like a shallow donor.[14] However, the O-H donors are unstable and decay completely at room temperature.[15] The characteristic time scale of this process is consistent with the observed instability of the Mn^{2+} resonance. Hence, a likely microscopic mechanism to account for the appearance of the Mn^{2+} resonance upon hydrogenation must be coupled to the introduction of additional free electrons from the H shallow donors. In the as-grown state, Mn would be in the Mn^{3+} charge state. Upon hydrogenation, an electron is captured into the Mn d orbitals changing its charge state to Mn^{2+} and hence the characteristic lines appear. Unfortunately, the Mn d orbitals reside close to the valence band, and the presence of Mn^{3+} would imply a Fermi energy below $E_V + 0.9\,\text{eV}$. Such a low Fermi energy is hardly consistent with the doping asymmetry of ZnO, which exclusively favors electron conduction. Hence, the Mn^{3+} charge state should not be stable. To elucidate this contradiction, density functional theory calculations were performed.

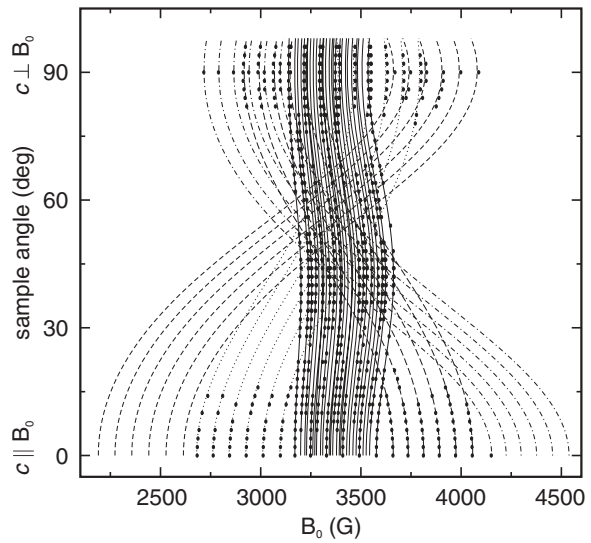

FIG. 2. EPR rotational pattern of Mn^{2+} traces in hydrogenated ZnO. Measured transitions are marked by solid points. Lines denote simulated resonance positions calculated from Eq. (1). Lines of equal style correspond to hyperfine transitions of the same electron spin transition.

III. COMPUTATIONAL METHODS

Spin-polarized charged-defect calculations on transition-metal complexes in zinc oxide were performed using a first-principles approach based on density functional theory (DFT). Transition metals substituting for the Zn lattice site were placed inside a 72-atom $3 \times 3 \times 2$ supercell. The calculations were performed with the Vienna Ab initio Simulation Package (VASP)[16,17] employing the generalized gradient approximation (GGA) in the formulation of Perdew, Burke, and Ernzerhof.[18] A Γ-centered $2 \times 2 \times 2$ k-point mesh and a plane-wave cutoff of 520 eV were used.

To improve the description of TM $3d$ electrons, the empirical on-site Coulomb correction (GGA + U) was used.[19] The necessary amount of correction U was systematically calculated for a number of $3d$ transition metals involving the screened atomic correlation energy[20] as proposed by Janotti *et al.*,

$$U = \frac{E(d^{n+1}) - E(d^n) - [E(d^n) - E(d^{n-1})]}{\varepsilon^{\infty}}. \qquad (2)$$

The electronic screening is expressed by the static dielectric constant $\varepsilon^{\infty} = 3.8$ while $E(d^n)$ denotes the total energy of an isolated transition-metal ion in a $3d^n$ electronic configuration. The resulting values for U are summarized in Table I. Except for Ti, the U parameter increases toward the half and filled $3d$ electron shell. This is consistent with an increasing correlation due to a larger number of parallel spin pairs from V to Mn and from Fe to Zn.

Charge transition levels were calculated from the energy of formation of the TM complex in different charge states. The GGA + U method was also used to calculate the scaling behavior of charge transition levels with respect to the

TABLE I. Calculated Coulomb parameter U for the correction of TM $3d$ electrons.

Transition metal	Ti	V	Cr	Mn	Fe	Co	Ni	Cu	Zn
U (eV)	2.8	2.0	2.2	3.2	2.2	2.5	2.6	2.7	4.7

band-gap error as described in Ref. 21. This formalism is well-suited for defects whose electronic states participating in charge transitions are isolated within the band gap and do not interact with the valence and conduction bands of ZnO. The transition metals from Cr to Ni fulfill this condition. Spurious hybridization and band-filling effects may reduce the accuracy of the calculations for Ti, V, and Cu. Since the band-gap correction is based on energy scaling, possible errors are expected to also scale with energy. Comparison of the calculated charge transition levels of isolated TMs in ZnO with experimental values suggests a relative error of less than 10%.

Finite-size effects due to the charged supercell approach were taken into account. The scaling behavior of an isolated charged TM defect was calculated for supercells of 72 up to 256 atoms and compared to the Madelung energy E_M of the respective superlattices. E_M typically overestimates the correction. Indeed, the supercell size effects were found to scale as $0.65 \times E_M$, which is in agreement with former results of Lany and Zunger.[22] Charge transition levels employing singly and doubly charged TM defects were corrected by 0.34 and 1.03 eV, respectively.

IV. RESULTS AND DISCUSSION

A. Isolated transition metals

Isolated transition metals span the entire range from donorlike, isoelectric, to even acceptorlike defects in ZnO. Figure 3 shows the calculated charge transition levels for transition metals of the iron group occupying a Zn lattice site.

Since the $2+/3+$ charge transition level of Ti and V resides close to or even inside the conduction band, the common charge state of these transition metals in natural n-type ZnO is the $3+$ charge state. Thus, one of their electrons has been transferred to the Fermi reservoir increasing the net concentration of free electrons. Indeed, the incorporation of Ti enhances the electrical conductivity of ZnO. This was experimentally observed for Ti ion-implanted ZnO nanowires[23] and was attributed to the donor character of Ti, which is in accordance with the calculated $2+/3+$ transition level. The $2+/3+$ charge transition of V resides inside the conduction band. According to our calculations, one of the $3d$ electrons of V relaxes to the conduction-band edge rendering V a shallow donor. EPR studies of V traces demonstrate that the stable charge state is indeed V^{3+}.[24] Hence, Ti and V play an active role in the charge-carrier balance of ZnO. Both are expected to enhance the dominating n-type conductivity of ZnO by direct donation of electrons to the Fermi reservoir.

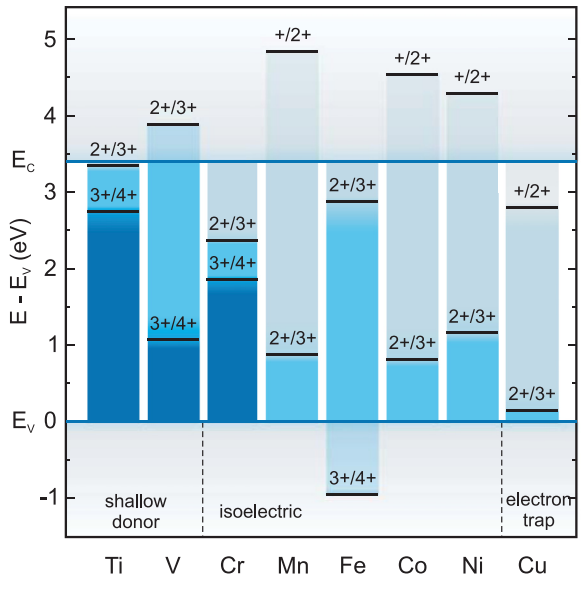

FIG. 3. (Color online) Stable charge states of isolated substitutional transition metals in ZnO. Donorlike charge transitions are labeled $2+/3+$ or $3+/4+$ and acceptorlike transitions are labeled $+/2+$.

Besides the donorlike elements Ti and V, the isovalent transition metals Cr, Mn, Fe, Co, and Ni do not directly contribute to the free-carrier concentration of ZnO. In n-type ZnO, where the Fermi energy resides near the conduction band, these elements are stable in the same $2+$ charge state as the Zn ions they substitute. However, they can be converted to their trivalent form depending on the Fermi level of ZnO. Fe converts to Fe^{3+} if the Fermi energy is below 2.9 eV. This is in accordance with results from magnetophotoluminescence measurements by Heitz *et al.*[25] In comparison to Mn, the donorlike $2+/3+$ transition of Fe resides much closer to the conduction band. This is due to the strong electronic correlation of the half-filled Mn $3d^5$ shell, while the unpaired spin-down electron of Fe $3d^6$ can be easily ionized.

In natural n-type ZnO, the Ni^{3+} charge state is unstable (Fig. 3). However, the conversion of Ni^{2+} to Ni^{3+} can be driven by the absorption of photons with an energy of $\geqslant$2.8 eV.[26] Assuming a transition into empty states of the conduction band, this can be interpreted as an optical transition level at $E_V + 0.6$ eV. Our calculation of the thermodynamic transition yields $E_V + 1.2$ eV. The energy difference between the optical and thermodynamic transition is attributed to the relaxation of atoms surrounding the trivalent ion. This effect is found to play a significant role for the thermodynamic charge transition levels of transition metals in ZnO.

The $2+/3+$ charge transition of Mn resides even closer to the valence band at $E_V + 0.9$ eV. That is why the Mn^{3+} charge state is unstable in natural ZnO. Hence, the hydrogen activation of the electron paramagnetic resonance of Mn observed for single-crystal ZnO cannot be explained by recharging of isolated Mn^{3+} ions.

B. Formation of Mn-O_i complexes

The charge transition levels of Mn strongly depend on the binding energy of the $3d$ electrons and hence on the electrostatic potential surrounding the Mn ion. With increasing electrostatic potential, the binding energy of the d electrons decreases. One possibility to affect the local electrostatic potential is the formation of complexes with charged defects. Hence, in the presence of compensated acceptors, such as interstitial oxygen, O_i, the energy of the $3d$ orbitals is raised above the Fermi energy. This stabilizes the Mn^{3+} charge state.

Interstitial oxygen bound to Mn exhibits a pair binding energy of $E_B = 1.6$ eV. Once an Mn-O_i complex is formed, it remains stable even at elevated temperatures. Furthermore, the formation of Mn-O_i is much more likely than the formation

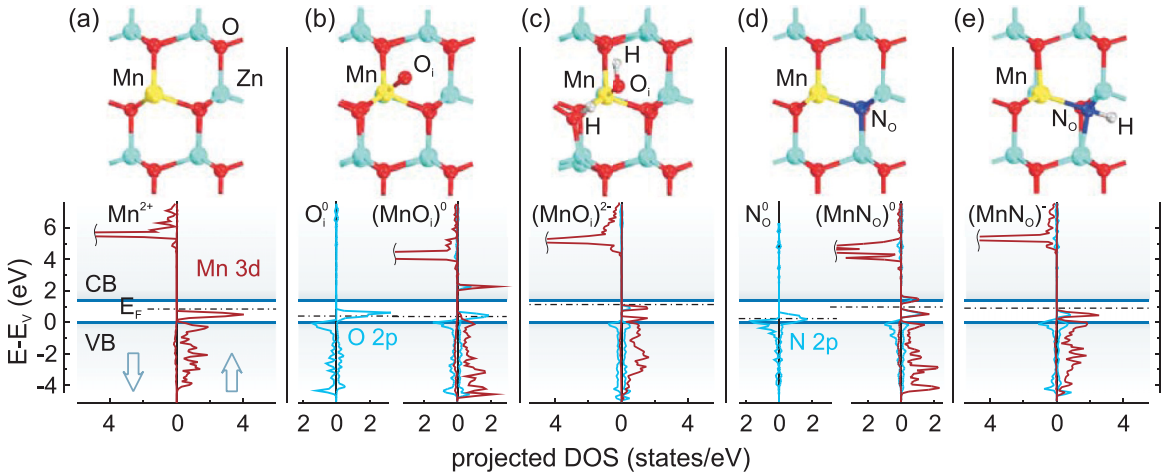

FIG. 4. (Color online) Upper panel: Structure of isolated Mn (a), MnO_i (b), MnO_i-2H (c), MnN_O (d), and MnN_O-H (c) complexes. Lower panel: Mn 3*d*- [dark gray (red)] and acceptor 2*p*-projected [light gray (blue)] density of states (DOS). The antibonding orbital of the complex is derived from Mn 3*d* states and resides above the conduction-band edge changing the Mn charge state to Mn^{3+} (b, d). Electrons of additional H donors occupy the 3*d* antibonding orbital restoring the Mn^{2+} charge state (c, e).

of an isolated oxygen interstitial. Isolated O_i has been studied in detail by Janotti *et al.* and the energy of formation varies between 8.5 eV for the neutral charge state in *p*-type Zn-rich conditions and 0.6 eV for the 2+ charge state in n-type O-rich conditions.[21] These values are reproduced by our calculation with a deviation of less than 5%. The same formalism applied to the Mn-O_i complex reveals much lower energy of formation. In contrast to isolated interstitial oxygen, Mn-O_i complexes will form in *p*-type Zn-rich conditions if 6.4 eV can be provided while at O-rich conditions even the neutral charge state exhibits negative energy of formation. Hence, Mn-O_i complexes form spontaneously if ZnO is grown at oxygen-rich conditions.

To understand the mechanism of TM–acceptor complex formation, Fig. 4 depicts the structure and the projected density of states (DOS) of substitutional Mn and its complexes with O_i, $O_i - 2H$, N_O, and $N_O - H$. The isolated Mn defect [Fig. 4(a)] causes only little distortion of the surrounding ZnO lattice, since its ionic radius is similar to that of Zn. The adjacent shell of O atoms relaxes outward by 4.4% of the regular Zn-O bond length. In the second next-neighbor Zn shell, the deformation is already reduced to 1.4%. Hence, defect strain is easily released, which results in a high solubility limit of 25 mol % for Mn in ZnO.[27]

The Mn ion mimics the nearly ionic binding of the ZnO host by transferring the valence 4*s* electrons to the surrounding O neighbors. The highest occupied levels are 3*d* spin-up states located in the band gap and are partly in resonance with the valence band [Fig. 4(a)]. The empty spin-down band is located 5.9 eV above the valence-band edge, which places it inside the conduction band. This results in the stability of the Mn^{2+} charge state. Consequently, in defect-free Mn-doped ZnO, the Mn^{2+} EPR spectrum should be observable.

However, intrinsic defects such as O_i are common in ZnO. These acceptors readily bond to substitutional transition metals. In the case of Mn, the Mn-O_i distance is 12% shorter than the respective Zn-O_i distance. This indicates the formation of a bond that changes the electronic structure of both components. One of the Mn 3*d* spin-up orbitals hybridizes with an O 2*p* level. This leads to the formation of a bonding and an antibonding orbital. The bonding orbital is filled with the Mn 3*d* electron while the antibonding orbital resides in the conduction band and is empty [see Fig. 4(b)].

For heterogeneous complexes, the electronegativity determines the character of bonding and antibonding orbitals. The difference in electronegativity between O and Mn amounts to 2.0 and is even larger than the difference between O and Zn of the neutral Mn-O_i complex. The resulting single-electron states can be seen in the Mn 3*d* and O 2*p* projected DOS in Fig. 4(b). Since O is more electronegative than Mn, the bonding orbital of the Mn-O_i complex is mostly derived from the O 2*p* levels, while the antibonding orbital originates from the Mn 3*d* orbitals. This is an interesting result with implications for both complex partners. On the one hand, the formation of the acceptor complex effectively shifts one of the Mn spin-up 3*d* levels to the conduction band. Consequently, the electron of this *d* orbital is transferred to the 2*p* orbital of the O_i acceptor leaving the Mn atom in the Mn^{3+} charge state. Hence, the shallow acceptor acts as a deep electron trap. According to the experimental observation of the hydrogen donor activated Mn EPR, the lack of an Mn^{2+} resonance in as-grown ZnO could be due to the presence of Mn-O_i complexes. When H is introduced, interstitial as well as lattice O atoms can capture H atoms forming O-H donors [Fig. 4(c)]. O_i is a double acceptor. Hence, one electron of the H donors relaxes into the second empty acceptor orbital. Since the concentration of H donors exceeds the Mn content by approximately four orders of magnitude, plenty of free electrons are available to additionally occupy the antibonding orbital [Fig. 4(c)]. Since this is a *d* orbital originating from the Mn atom, the additional electron changes the Mn charge state to Mn^{2+} rendering it EPR-active.

This recharging mechanism is not limited to interstitial oxygen. Besides the interaction with intrinsic acceptors, the Mn^{3+} charge state can also be stabilized by complex formation with extrinsic acceptors. The Mn complex with substitutional nitrogen depicted in Fig. 4(d) shows the same characteristics.

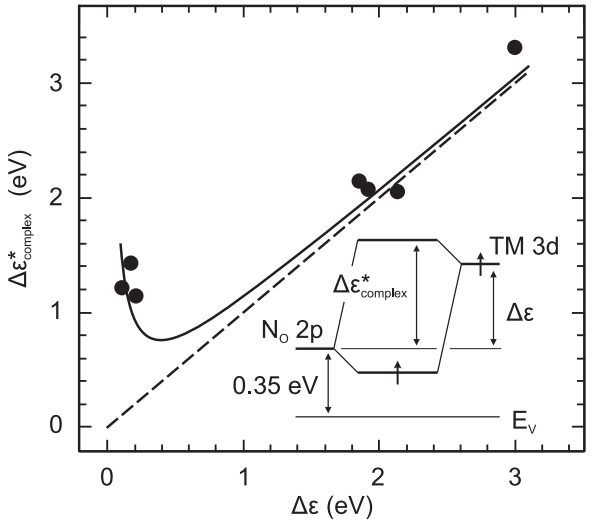

FIG. 5. Energetic distance $\Delta\varepsilon^*_{complex}$ of the antibonding complex orbital to the $2p$ orbital of the N_O acceptor as a function of the energetic position of the TM $3d$ levels. The inset illustrates the TM-N_O bond formation. The solid line is a fit to the data according to Eq. (3) with $|\beta| = 0.38$ eV. The dashed line corresponds to $\beta = 0$.

As in the case of Mn-O_i, the charge transfer from the TM $3d$ state into the nitrogen $2p$ level stabilizes the Mn^{3+} charge state by shifting the antibonding orbital toward the conduction-band edge. At the same time, the nitrogen acceptor is compensated. In contrast to the O_i acceptor, substitutional N_O is a single acceptor. Hence, only one donor electron is needed to fill the Mn $3d$ antibonding orbital and convert Mn into the $2+$ charge state upon hydrogenation [see Fig. 4(e)].

C. Transition-metal acceptor complexes

Besides the stabilization of uncommon TM charge states, complex formation also affects the acceptor. The mechanism of acceptor compensation with TMs is a universal process. All complexes of nitrogen with TMs from titanium to copper show a similar behavior. In Fig. 5, the energetic distance of the antibonding orbital of the TM-N_O complex and the N acceptor orbital, $\Delta\varepsilon^*_{complex}$, is plotted as a function of the alignment of the TM $3d$ and nitrogen $2p$ orbitals, $\Delta\varepsilon$ (see the inset). Each data point corresponds to the highest occupied and lowest empty $3d$ level of a TM deduced from the density of states before and after complex formation. According to the linear combination of atomic orbitals (LCAO) theory of heterogeneous complexes in the Mulliken approximation, the energy of the antibonding complex orbital is a function of $\Delta\varepsilon$ and the resonance integral β.[28] In the case of small β, it can be approximated by

$$\Delta\varepsilon^*_{complex} \approx \Delta\varepsilon + \frac{\beta^2}{\Delta\varepsilon} + \cdots . \quad (3)$$

Assuming that β is similar for all investigated TMs, the data in Fig. 5 were fitted to Eq. (3) and yielded $|\beta| = 0.38$ eV (full curve in Fig. 5). Since β^2 enters Eq. (3), only the absolute value of the resonance integral can be deduced. However, β is typically found to be negative. For transition metals with donor character, where $\Delta\varepsilon > |\beta|$, acceptor compensation occurs by a transfer of $3d$ electrons into the nitrogen $2p$ orbitals.

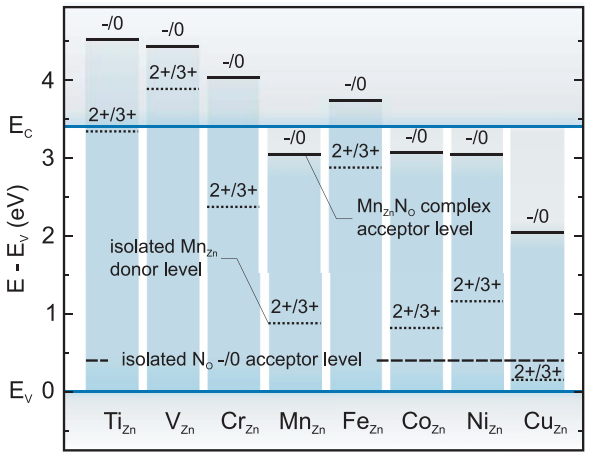

FIG. 6. (Color online) Charge transition levels of TM_{Zn}-N_O complexes. Dashed and dotted lines show the levels of the isolated N_O and TM_{Zn}, respectively.

Hence, the electron accepting orbital is shifted by $\approx\Delta\varepsilon$. On the other hand, when $\Delta\varepsilon < |\beta|$, the acceptor orbital of the complex is shifted upward by the formation of a strong bond. Hence, when transition metals are incorporated into ZnO, they either act as donors or form TM-acceptor complexes. Both mechanisms cause a decrease of the acceptor doping efficiency. With regard to the DMS concept based on p-type ZnO, it is impossible to incorporate a high concentration of Mn atoms and simultaneously achieve a high hole concentration that is necessary to attain a Curie temperature above 300 K.

Based on the single-electron orbital picture, the charge transition levels of the acceptor complexes were calculated, and corrections for the band-gap error were applied. The results are shown in Fig. 6. For every transition metal, the acceptor level of the TM-N_O complex resides above the donor level of the isolated TM and above the N_O acceptor level. The effective shift of the acceptor level is small for donorlike transition metals (e.g., Ti, V, and Fe), since the electron is simply transferred from the transition metal to the nitrogen acceptor. In the case of isovalent transition metals (e.g., Mn, Co, and Ni), the shift is significantly larger since compensation is mediated by the formation of a bond. Interestingly, the transition level of copper resides below the nitrogen acceptor level. For isolated Cu and N_O, a charge transfer is not expected. However, if a Cu-N_O complex is formed, the acceptor level shifts toward the conduction band by about 1.5 eV.

The acceptor compensation mechanism reveals a major flaw in the concept of hole-mediated ferromagnetism in ZnO. The presence of transition metals in the vicinity of acceptors causes the annihilation of holes that are required to mediate the spin-spin interaction. At the same time, the amount of unpaired spins and hence the maximum attainable magnetization is reduced; e.g., the magnetization decreases from $5\mu_B$ per ion in Mn^{2+} to $4\mu_B$ per ion in Mn^{3+}, where μ_B is the Bohr magneton.

V. SUMMARY

We have shown that additional electrons introduced by H shallow donors change the charge state of Mn from Mn^{3+} to Mn^{2+}. This gives rise to a fine and hyperfine

split electron paramagnetic resonance. However, the Mn 3*d* orbitals reside close to the valence band and should always be occupied. Hence, the Mn^{3+} charge state should not be stable. DFT calculations were performed to elucidate this contradiction. They show that Mn readily forms complexes with O_i and N_O transferring charge carriers from the TM to the acceptor. Hence, the TM charge state changes to Mn^{3+}. A subsequent hydrogenation renders the Mn atoms EPR-active. The acceptor compensation mechanism is not limited to Mn. Similar behavior was observed for all TMs from Ti to Cu. This mechanism reveals a major flaw in the concept of hole-mediated ferromagnetism in ZnO.

[1] S. A. Wolf, D. D. Awschalom, R. A. Buhrman, J. M. Daughton, S. von Molnár, M. L. Roukes, A. Y. Chtchelkanova, and D. M. Treger, Science **294**, 1488 (2001).

[2] T. Dietl, H. Ohno, F. Matsukura, J. Cibert, and D. Ferrand, Science **287**, 1019 (2000).

[3] Z. W. Liu, C. K. Ong, T. Yu, and Z. X. Shen, Appl. Phys. Lett. **88**, 062508 (2006).

[4] D. L. Hou, X. J. Ye, H. J. Meng, H. J. Zhou, X. L. Li, C. M. Zhen, and G. D. Tang, Appl. Phys. Lett. **90**, 142502 (2007).

[5] S. A. Chambers, Adv. Mater. **22**, 219 (2010).

[6] H. Gu, Y. Jiang, Y. Xu, and M. Yan, Appl. Phys. Lett. **98**, 012502 (2011).

[7] C. D. Pemmaraju, R. Hanafin, T. Archer, H. B. Braun, and S. Sanvito, Phys. Rev. B **78**, 054428 (2008).

[8] A. Tsukazaki, A. Ohtomo, T. Onuma, M. Ohtani, T. Makino, M. Sumiya, K. Ohtani, S. F. Chichibu, S. Fuke, Y. Segawa, H. Ohno, H. Koinuma, and M. Kawasaki, Nat. Mater. **4**, 42 (2005).

[9] D. M. Hofmann, A. Hofstaetter, F. Leiter, H. Zhou, F. Henecker, B. K. Meyer, S. B. Orlinskii, J. Schmidt, and P. G. Baranov, Phys. Rev. Lett. **88**, 045504 (2002).

[10] A. Hausmann and H. Huppertz, J. Phys. Chem. Solids **29**, 1369 (1968).

[11] M. A. Gluba, F. Friedrich, K. Lips, and N. H. Nickel, Superlatt. Microstruct. **43**, 24 (2008).

[12] S. Stoll and A. Schweiger, J. Magn. Reson. **178**, 42 (2006).

[13] E. Chikoidze, H. J. von Bardeleben, Y. Dumont, P. Galtier, and J. L. Cantin, J. Appl. Phys. **97**, 10D316 (2005).

[14] C. G. Van de Walle, Phys. Rev. Lett. **85**, 1012 (2000).

[15] S. J. Jokela and M. D. McCluskey, Phys. Rev. B **72**, 113201 (2005).

[16] G. Kresse and J. Furthmüller, Phys. Rev. B **54**, 11169 (1996).

[17] G. Kresse and D. Joubert, Phys. Rev. B **59**, 1758 (1999).

[18] J. P. Perdew, K. Burke, and M. Ernzerhof, Phys. Rev. Lett. **77**, 3865 (1996).

[19] A. I. Liechtenstein, V. I. Anisimov, and J. Zaanen, Phys. Rev. B **52**, R5467 (1995).

[20] A. Janotti, D. Segev, and C. G. Van de Walle, Phys. Rev. B **74**, 045202 (2006).

[21] A. Janotti and C. G. Van de Walle, Phys. Rev. B **76**, 165202 (2007).

[22] S. Lany and A. Zunger, Phys. Rev. B **78**, 235104 (2008).

[23] L. Liao, Z. Zhang, Y. Yang, B. Yan, H. T. Cao, L. L. Chen, G. P. Li, T. Wu, Z. X. Shen, B. K. Tay, T. Yu, and X. W. Sun, J. Appl. Phys. **104**, 076104 (2008).

[24] P. Schreiber and A. Hausmann, Zeitschrift für Physik **251**, 71 (1972).

[25] R. Heitz, A. Hoffmann, and I. Broser, Phys. Rev. B **45**, 8977 (1992).

[26] W. C. Holton, J. Schneider, and T. L. Estle, Phys. Rev. **133**, A1638 (1964).

[27] C. Bates, W. White, and R. Roy, J. Inorg. Nucl. Chem. **28**, 397 (1966).

[28] P. Atkins and J. de Paula, *Physical Chemistry*, 8th ed. (Freeman and Company, New York, 2006).